SHEAR OR BENDING? EXPERIMENTAL RESULTS ON LARGE T-SHAPED PRESTRESSED CONRETE BEAMS

Ir. S.W.H Ensink
Delft University of Technology
Faculty of Civil Engineering
& Geosciences
The Netherlands

Dr.ir. C. van der Veen
Delft University of Technology
Faculty of Civil Engineering
& Geosciences
The Netherlands

Dr.ir. A. de Boer
Ministry of Infrastructure and the Environment
The Netherlands

KEYWORDS: experiment; prestressed concrete; T-shaped beam; bridge girder; shear; contest; non-linear analysis.

ABSTRACT

Experimental results of four shear tests on two large prestressed concrete beams are compared to non-linear analysis and design code calculations. The beams have a length of 12 m and a depth of 1.3 m and are reinforced with stirrups and pre-tensioning. The four tests consist of a single point load at a distance of 2.7d from the support. A priori analyses using NLFEA and design formula predicted a shear failure. However a bending moment failure was predicted to be close to the shear failure and could not be completely ruled out. The prediction of shear or bending failure is further complicated by the presence of empty ducts in the top flange. The four test where the subject of an international “Shear Contest” held at the University of Parma Italy in November 2014.

INTRODUCTION

The cross-sections of the beams are a 1:2 scale model of the approach bridge of the Van Brienenoord bridge in Rotterdam (the Netherlands), see figure 1. The reinforcement and prestressing was designed with requirements of a previous experiment. This previous experiment consisted of four beams with cast in between slabs, transverse end beams and transverse prestressing. The ultimate limit state behaviour of the slabs was the aim of this previous experiment so the beams were over dimensioned. After these experiments were completed, it was decided to conduct shear tests on the beams themselves. The location of the point load at 2.7d from the support was based on a preliminary non-linear analysis [2] predicting a shear failure.

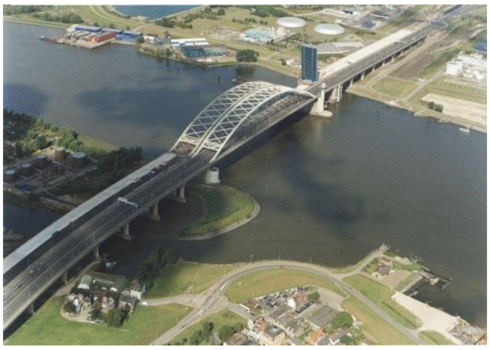

(a)

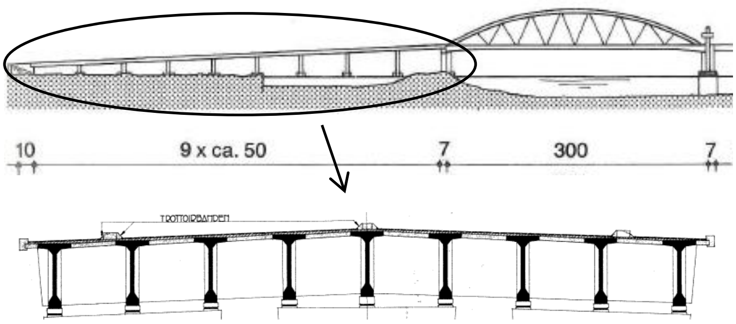

(b)

Fig. 1 Van Brienenoord Rotterdam areal view (a) approach bridge with cross-section (b)

BEAM PROPERTIES

The T-shaped beams, with a length of 12 m and a depth of 1.3 m, have been prefabricated in a factory. Figure 2 shows the symmetric half-length of the beam with the cross-sections shown in figure 3b. Type 101 and type 201 beam differ in the width of the top flange (750 mm versus 875 mm). Since type 201 beam has a wider flange on one side the cross-section of this beam is non-symmetric.

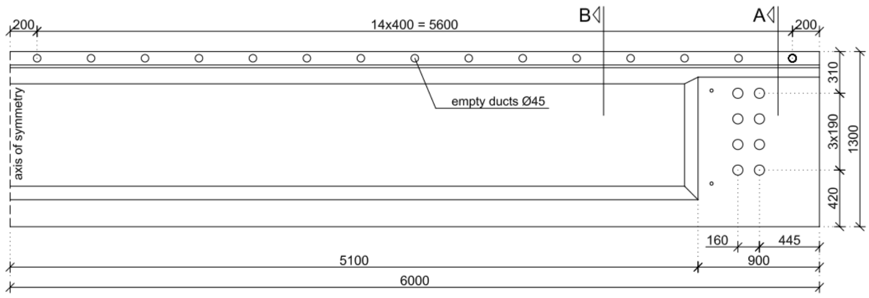

Fig. 2 Side view beam type 101 & 201

Empty ducts used for transverse prestressing in the previous experiments are present in the top flange (Ø45 mm c.t.c. 400 mm) and at the end blocks (8× Ø65 mm). Figure 3a shows the shear reinforcement with stirrups Ø10 mm at an average distance of 114 mm and the reinforcement in the top and bottom flanges. The beams are pre-tensioned using 24 strands Ø15.7 mm with steel type FeP1860. The prestressing force per strand is ~196 kN (measured force per strand ~214 kN reduced with effect of elastic deformation).

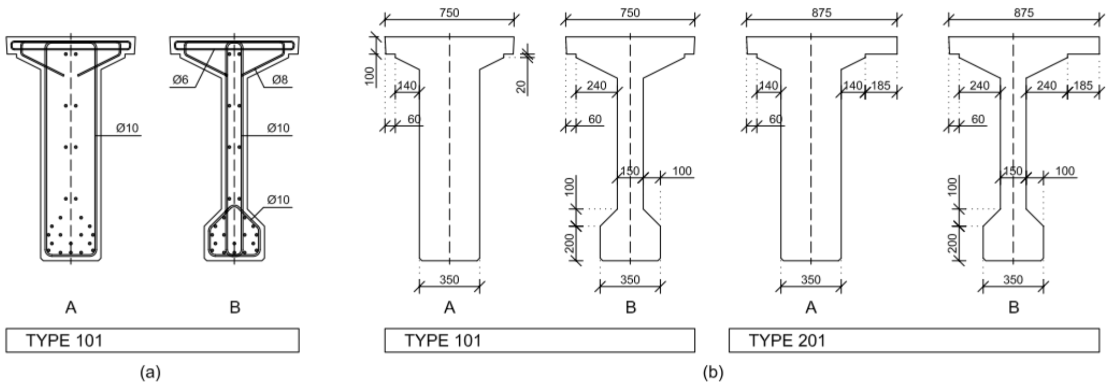

Fig. 3 Layout prestressing strands and shear reinforcement (a) cross sections A/B (b)

The (self-compacting) concrete type is C53/65. The mean cubic compressive strength at the time of prestressing was determined at $f_{cm,cube}$ = 54 N/mm^2. After 28 days the strength has increased to $f_{cm,cube}$ = 83 N/mm^2 ($f_{ck,cube}$ = 77 N/mm^2). After 273 days and again just before the start of the beam experiments, at an concrete age of 871 days, three 150×150×150 mm^3 cubes have been tested in compression (C) and splitting (S), the results are given in table 1.

Table 1 Results of cube tests

number	test	$f_{cm,cube}$ [N/mm^2]	$f_{ctm,sp}$ [N/mm^2]	age [days]	number	test	$f_{cm,cube}$ [N/mm^2]	$f_{ctm,sp}$ [N/mm^2]	age [days]
1	C	89.92		273	7	C	89.20		871
2	C	91.62		273	8	C	87.86		871
3	C	87.95		267	9	C	102.69		871
4	S		6.15	273	10	S		7.52	871
5	S		6.37	273	11	S		8.01	871
6	S		6.39	273					

Disregarding the result of compression test number 9, which shows an unusual high value, no significant increase in compressive strength was found between the age of 273 days as compared to the age of 871 days. However, the splitting test does suggest an increase in tensile strength of about 23%.

Steel reinforcement (stirrups Ø10) was removed and tested after the experiments resulting in a mean yielding strength of f_{yk} = 547 N/mm^2 and a mean ultimate strength of f_{tk} = 635 N/mm^2. Furthermore, one of the tests indicated that the stirrup had already yielded during the experiment.

EXPERIMENTAL SETUP

In all experiments the center of the loading jack is positioned at a distance of 2950 mm from the center of the support (2.7d) see figures 4 and 5. The dimensions of the loading jack are 250×250 mm whereas the dimensions of support plates are 350×280 mm (support type A/B). Therefore the width of the support plate is equal to the width of the beam. The position of the load means the edge of the loading jack is slightly overlapping one of the empty ducts by 25 mm.

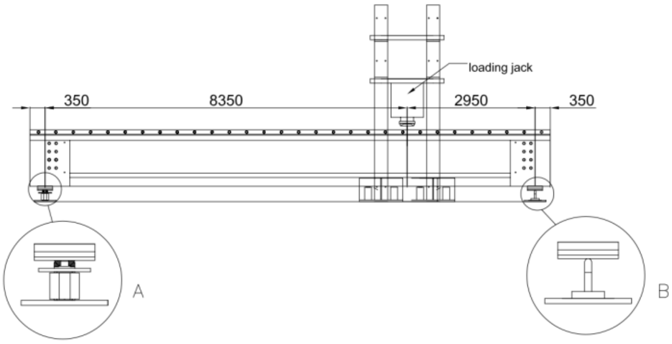

Fig. 4 Position of the load and supports


Fig. 5 Overview of test setup (first test beam 201)

Each beam is tested at both ends. After the first test of a beam is completed, although now largely damaged, the prestressing still prevents a complete fracture of the beam. To resist the forces of the second test the damaged area is outfitted with a support frame consisting of steel beams and vertical prestressing, see figure 6. In order to prevent excessive rotation or horizontal movement during testing a support frame with rollers is also fitted at both ends close to the top flange, see figure 7.


Fig. 6 Support frame with vertical prestressing

Fig. 7 Horizontal support at end of beam

Measurements include displacements at the position of the load and at the supports on both sides of the beam using lasers, the reaction forces at the supports using load cells and the force and displacement of the loading jack. The loading jack is displacement controlled and paused during the experiment at certain fixed load levels to record the crack development and measure the crack width.

TEST RESULTS

Beam type 101

A previous experiment [1] on this beam involved a single point load at 3 positions close to the centre of the beam. These experiments were conducted when this beam was part of a larger setup consisting of four beams with cast in between slabs, transverse end beams and transverse prestressing. As a result of this previous experiment bending cracks are present over a large area (~3m). However, due to the amount of prestressing these cracks have mostly closed again. Also a relatively low force was applied (1950 kN of which a maximum of 1050 kN was taken by this beam and the rest by the neighbouring beams). It is therefore expected that this “weak spot” at the centre of the beam will not have a significant influence during the shear tests which are much closer to the support. Figure 8 shows the load versus displacement of the tests on beam type 101.

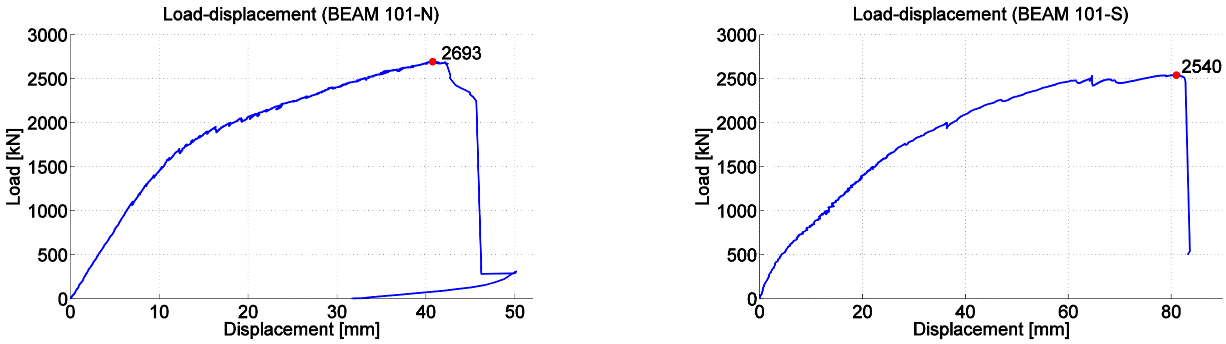

(a) North side (first test) (b) South side (second test)

Fig. 8 Load-displacement beam type 101

The displacements of the second test are much larger due to the “weak spot” created by the first test which is reinforced by the support frame (see also figure 6). This implies an insufficient stiffness of the support frame. The crack development from the first test is shown in figure 9. The measured crack width is given in table 2. The first bending cracks (hairline cracks) are visible at a load of 1700 kN. Next horizontal shear cracks occur in the web between the load and the support just below the top flange. Finally inclined shear cracks occur in the web that fan out at different angles towards the support. Also at a relatively low load level (1900 kN) a large vertical bending crack was observed in the web. This indicates that although the load is close to the support still a relatively large bending moment is present. The crack development of the second test is consistent with the first test and shows a similar crack pattern at equal load levels.

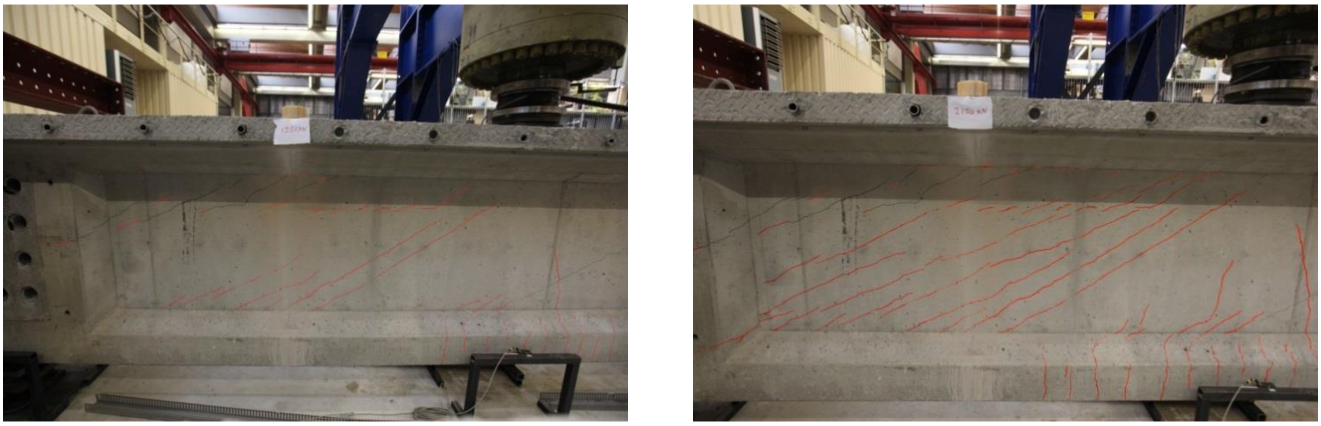

(a) 1950 kN (b) 2150 kN

Fig. 9 Crack development beam type 101 (first test)

Table 2 Crack width beam type 101

North side (first test)			South side (second test)		
load [kN]	crack width (shear) [mm]	crack width (bending) [mm]	load [kN]	crack width (shear) [mm]	crack width (bending) [mm]
2050	0.05-0.10	0.10	1850	-	0.05
2100	0.15	0.20	1900	-	0.10-0.15
2150	0.05-0.15	0.30	1950	-	0.10-0.15

The average crack spacing at ULS is measured from a large number of bending cracks and a limited number, i.e. four, shear cracks. For the first test an average crack spacing is found of 128.4 mm (bending) and 98.8 mm (shear). For the second test an average crack spacing is found of 140.8 mm (bending) and 63.8 mm (shear).

The fracture of the beam is shown in figure 10. Close to the failure load considerable crushing of the concrete near the empty ducts as well as flattening of the ducts themselves was observed (figure 10b). Of course this introduces a significant reduction of the capacity of the compression zone in the top flange. This phenomenon ultimately causes a bending moment like localized failure of the beam. The fracture of the second test is very similar to the first test.

(a) side view

(b) top view

Fig. 10 Failure of beam type 101 (first test)

Beam type 201

This beam has no existing cracks from previous experiments. In an attempt to prevent a premature failure of the compression zone three of the empty ducts at the position of the load are now filled with steel rods Ø40 mm see figure 11. The assumption is that the gap between the rods and the ducts will close at high load levels to create a continuous compression zone. Also the support frame used for the second test is strengthened with additional vertical prestressing (12× 100 kN), see figure 12 in relation to figure 6. Figure 13 shows the load versus displacement of the tests on beam type 201.

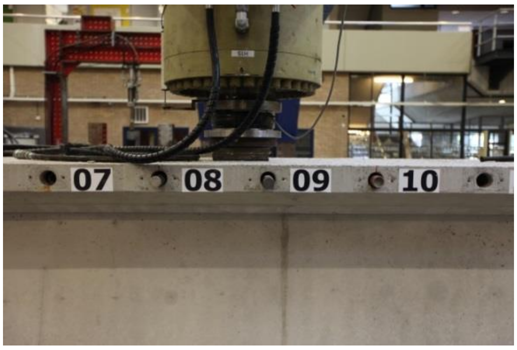

Fig. 11 Ducts in top flange filled with steel rods

Fig. 12 Support frame with additional vertical prestressing

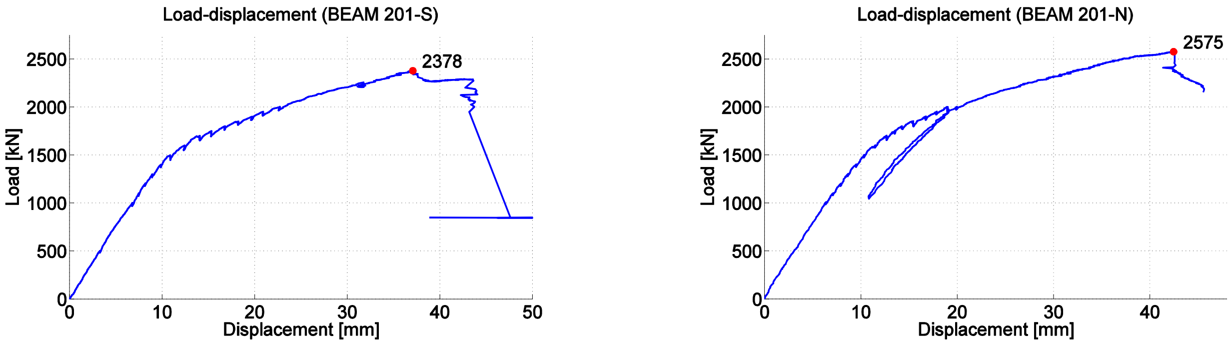

(a) South side (first test) (b) North side (second test)

Fig. 13 Load-displacement beam type 201

Note that figure 13b shows an unscheduled unloading that has not affected the results of the test. As a result of the higher stiffness of the improved support frame the second test is now showing very similar displacements as the first test.

The crack development of the first test is shown in figure 14. The measured crack width is given in table 3. In this case the crack development of the second test is not consistent with the first test. In the first test, at 1500 kN, first horizontal shear cracks (hairline cracks) occur in the web between the load and the support just below the top flange, see figure 14a. Next bending cracks and inclined shear cracks occur almost simultaneously at a load of 1600 kN and continue to expand and grow until failure.

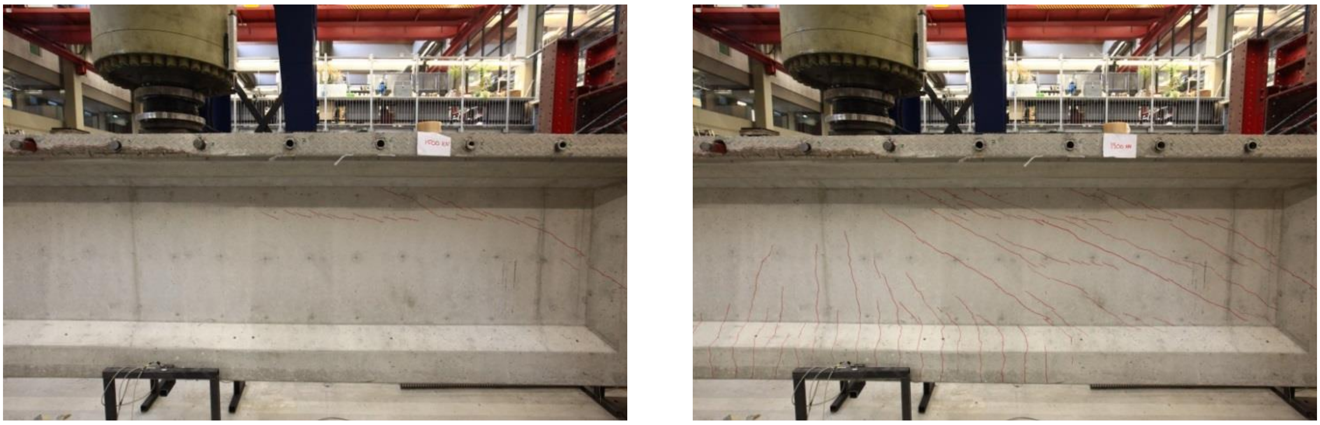
(a) 1500 kN (b) 1900 kN

Fig. 14 Crack development beam type 201 (first test)

In the second test, at 1700 kN, first horizontal shear cracks occur in the web between the load and the support near the bottom flange together with bending cracks and an inclined shear crack (hairline cracks), see figure 15a. After this initial cracking stage additional inclined shear cracks and bending cracks occur until failure. However, the inclined shear cracks in this test are much more localized in a narrow band at an angle that does not go all the way to the support, see figure 15b (picture taken after failure).

Table 3 Crack width beam type 201

South side (first test)			North side (second test)		
load [kN]	crack width (shear) [mm]	crack width (bending) [mm]	load [kN]	crack width (shear) [mm]	crack width (bending) [mm]
1800	0.15-0.20	0.05-0.10	1750	0.10	-
1850	0.20	0.05-0.10	1800	0.15	-
1900	0.25-0.30	0.20	1850	0.15	-
1950	0.30	0.20	1900	0.15	-
2000	0.35	0.20	1950	0.15-0.20	-

For the first test an average crack spacing is found of 118.6 mm (bending) and 97.5 mm (shear). For the second test an average crack spacing is found of 120.0 mm (bending) and 86.3 mm (shear).

(a) 1700 kN (b) 2000 kN

Fig. 15 Crack development beam type 201 (second test)

Although the empty ducts were now filled with steel rods still a localized failure of the compression zone occurred. However, much less crushing in the area near the ducts is observed. Because this beam is non-symmetric a significant rotation and horizontal deflection of the beam was observed during the tests. As a result of this rotation the "wide flange side" of the beam is much less damaged, compare figures 16a to 16b. The effect of the rotation is also plotted in figure 16c (taken from a cross-sectional analysis) showing much higher compressive strains on the "narrow flange side".

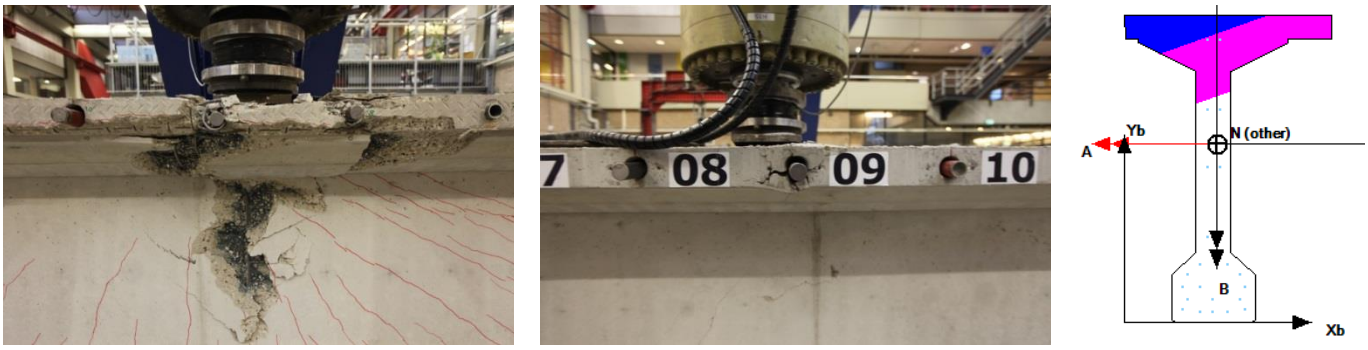

(a) Narrow flange side (b) Wide flange side (c) strains

Fig. 16 Failure of beam 201 (first test) and strain plot from cross-sectional analysis

FINITE ELEMENT ANALYSIS

The four experiments where the subject of an international "Shear Contest" organised by the DIANA Users Association in collaboration with the Delft University of Technology, the Dutch Ministry of Infrastructure and the Environment and the University of Parma Italy. For this contest the participants were asked to make use of the "Guidelines for Nonlinear Finite Element Analysis of Concrete Girders" [3]. The goal was to predict the failure load as close as possible and to verify that this guideline is also acceptable for a larger group of international end-users and other software packages. The results of the experiments and the predictions where later presented at the University of Parma in November 2014.

In preparation of the experiments, at the proposed position of the load, a preliminary non-linear analysis [2] using the program ATENA [6] predicted a shear type failure and an ultimate failure load of 2416 kN. Because the experiments where aimed at a shear failure this analysis was used to determine the position of the load at 2.95 m from the support. Next a more detailed non-linear analyses using DIANA [7] as part of the aforementioned contest and following the “best practices” from the guideline was performed. Figure 17a shows part of the 3D FEM model (beam type 101) including the load and support plates. The stirrups, splitting reinforcement, longitudinal reinforcement and prestressing tendons were modelled using embedded reinforcement, see figure 17b. The empty ducts were not included in the model.

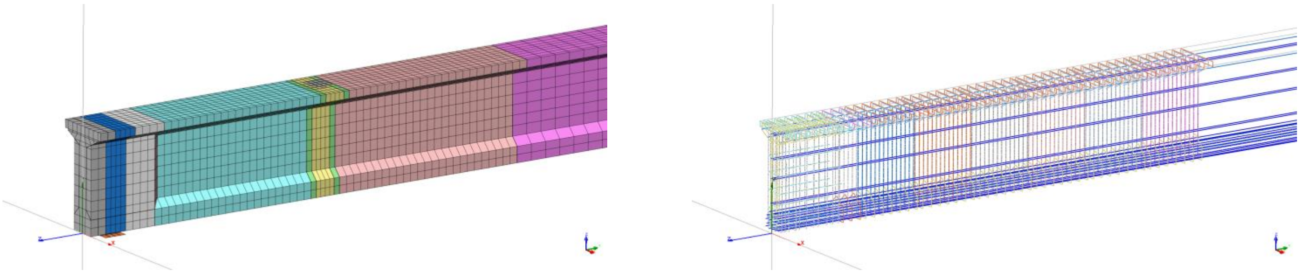

(a) (b)

Fig. 17 FEM model beam type 101 mesh (a) embedded reinforcement (b)

For the concrete a total strain rotating crack model and non-linear Hordijk tension softening was used. Furthermore, the material model uses a parabolic compression diagram and the influence of lateral cracking (tension-compression) is taken into account. Also a constant Poisson’s ratio, i.e. no decrease with cracking, is used. The steel reinforcement and the tendons both use an elasto-plastic stress-strain diagram with strain hardening. The main physical properties used in the FEM calculation are given in table 4.

Table 4 FEM material properties

Concrete			
mean compressive strength	f_{cm}	77	N/mm^2
mean tensile strength[1)]	f_{ctm}	5.67	N/mm^2
fracture energy	G_f	0.1565	Nmm/mm^2
compressive fracture energy	G_c	38.55	Nmm/mm^2
Poisson’s ratio	υ	0.15	-
Young’s modulus[2)]	E_c	34475	N/mm^2
Steel reinforcement			
assumed mean yielding strength[3)]	f_{ym}	540	N/mm^2
assumed ultimate tensile strength[3)]	f_{tk}	620	N/mm^2
Poisson’s ratio	υ	0.3	-
Young’s modulus	E_s	200000	N/mm^2
ultimate strain	ε_{uk}	5.0	%
Prestressing steel			
assumed 0.1% proof stress[3)]	$f_{p0,1k}$	1655	N/mm^2
assumed ultimate tensile strength[3)]	f_{pk}	1953	N/mm^2
Poisson’s ratio	υ	0.3	-
Young’s modulus	E_p	195000	N/mm^2
ultimate strain	ε_{uk}	3.5	%

[1)] $f_{ctm} = 0.9 \times 6.30 = 5.67$ N/mm^2 (average from splitting tests at age of 273 days)
[2)] reduced with a reduction factor equal to 0.85 to account for initial cracking due to creep, shrinkage etc. according to guideline [3]
[3)] based on past experimental results

Figure 18 shows the load-displacement curve of the non-linear calculation. The calculated failure load is 2348 kN and the deviation from the experiments is therefore 11%.

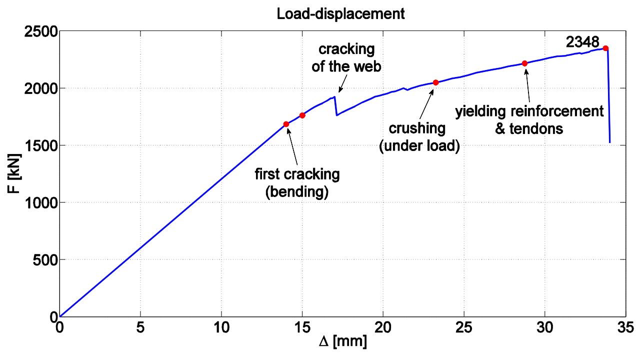

Fig. 18 Load-displacement non-linear analysis (beam type 101)

In the analysis, close to the failure load, simultaneous yielding of the stirrups and tendons is observed. However, the maximum shear capacity of the beam is not reached because the beam prematurely fails in bending. This was observed in the last load steps where the four tendons near the top flange started yielding (see also figure 3a). The principal total strain at three load levels is plotted in figure 19. The yellow/red parts of figure 19 indicate fully open cracks. The crack pattern found in the non-linear analysis is in good agreement with the crack pattern from the experiments.

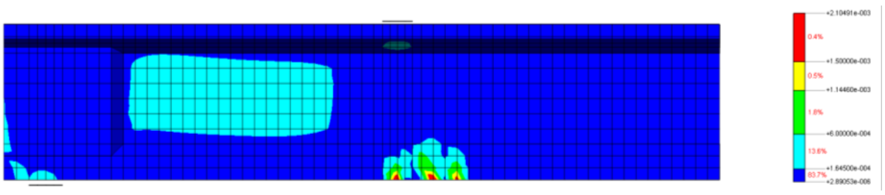

(a) u = 15.000 mm, F = 1767 kN

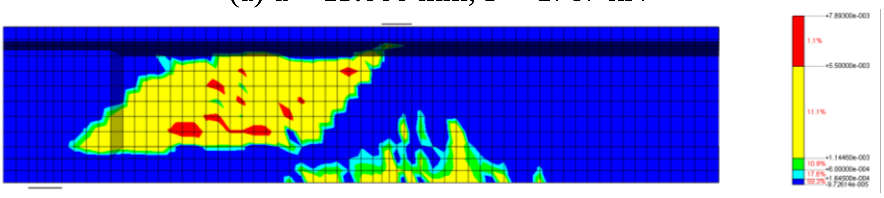

(b) u = 21.500 mm, F = 1984 kN

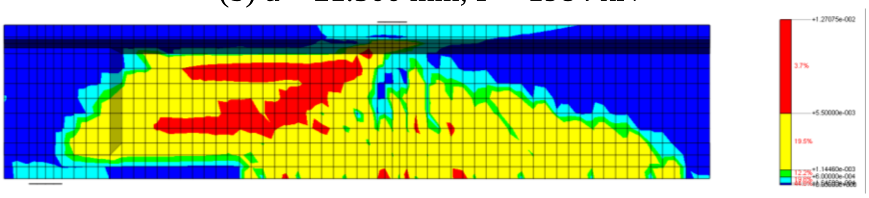

(c) u = 33.875 mm, F = 2348 kN

Fig. 19 Principal total strain

Because a rotating crack model was used, a lower bound failure load was expected to be found. However, according to the guideline [3] using a fixed crack model could lead to a considerable overestimation of the failure load. On the other hand, the empty duct where not part of the model which will presumably lead to a lower failure load. Although a reasonably fine mesh was used, the use of quadratic elements will be part of a future investigation as well as fixed crack models in combination with an adequate shear retention model.

DESIGN FORMULA

In this section the shear strength is calculated according to Eurocode 2 [4,5] using the mean value for concrete compressive strength (f_{cm} = 76 N/mm^2) and the mean ultimate tensile strength of the shear reinforcement (f_{tk} = 635 N/mm^2). The angle for the compression strut is taken as: tan θ = 1300/2950 → θ = 23.8^0. Furthermore, the average compressive stress is: σ_{cp} (t=882 days) = 11.94 N/mm^2 → α_{cw} = 1.16. The effective depth of the cross-section is taken as d = 1095 mm.

<u>Beam 101 (shear)</u>

Resistance of the shear reinforcement:

$$V_{Rd,s} = \frac{A_{sw}}{s} z f_{ywd} \cot\theta = \frac{157}{114.3} \cdot 0.9 \cdot 1095 \cdot 635 \cdot \cot 23.8 = 1949 \cdot 10^3 N = 1950\ kN$$

Resistance of the compression strut:

$$\begin{aligned} V_{Rd,max} &= \alpha_{cw} b_w z v_1 f_{cd} / (\cot\theta + \tan\theta) \\ &= 1.16 \cdot 150 \cdot 0.9 \cdot 1095 \cdot 0.6 \cdot \left(1 - \frac{76}{250}\right) \cdot 76/(\cot 23.8 + \tan 23.8) = 2004 \cdot 10^3\ N \\ &= 2004\ kN \end{aligned}$$

Note that for θ = 23.45 the resistance of the stirrups equals the resistance of the compression strut, i.e. $V_{Rd,s} = V_{Rd,max}$ = 1982 kN.

With the assumption of a fixed compression strut angle of θ = 23.8^0 the resistance of the stirrups $V_{Rd,s}$, reduced with the shear force of the dead weight (51 kN), translates to an applied load of approximately $F = (1950 - 51) \cdot 11.3/8.35 = 2570\ kN$. The deviation from the experiments is therefore 2%.

<u>Beam 101 (bending)</u>

Using the same physical properties as with the FEM analyses (see also table 4), an ultimate bending moment can be determined of 4100 kNm. The next step is to take into account the empty ducts in the top flange. Because the reduction of the compression zone is partly compensated by the favourable shift of the centre of gravity of the cross-section the ultimate bending moment reduces only slightly to 3871 kNm. However, the concrete compression zone height does increase significantly from 202 mm to 323 mm. Taking this into account as well as the bending moment from prestressing and the dead weight translates into an applied load of $F = 5358 \cdot 11.3/(2.95 \cdot 8.35) = 2458\ kN$.

<u>Beam 201 (shear/torsion)</u>

For the non-symmetric beam type 201 the load also introduces a torsional moment, which is resisted by the horizontal supports at the end of the beam, see figure 7. The centre of gravity of this beam is offset by just 15 mm. The constant torsional moment between the load and the support (see also figure 4) can be calculated by:

$$T = F \cdot z_x \cdot b/L = F \cdot 0.015 \cdot 8.35/11.3 = 0.0111 \cdot F$$

Furthermore approximately 70% of the torsion is assumed to be resisted by the web. Taking this into account and without the assumption of a fixed compression strut angle instead taking an optimum angle of θ = 23.5^0, i.e. $V_{Rd,s} = V_{Rd,max}$ = 1830 kN, results into an applied load of $F = (1830 - 53) \cdot 11.3/8.35 = 2405\ kN$ (the shear force of the dead weight is 53 kN). In this case the deviation from the experiments is 3%. For the combined shear/torsion capacity of the beam the effect of torsion on the unity check is limited to approximately 8%.

Beam 201 (bending)
The calculation of the ultimate bending moment for the non-symmetric cross-section is much more complicated and will be part of future investigation.

SUMMARY

Table 5 gives a summary of the results of the experiments, the NLFEA calculations and the design code and analytical calculations.

Table 5 Overview of experimental, FEA and design code / analytical results

Experiment	Beam 101 Load [kN]	Beam 201 Load [kN]
Experiment first test (bending failure)	2693	2378
Experiment second test (bending failure)	2540	2575
Average	**2617**	**2477**
NLFEA		
Preliminary 2D analysis (shear failure) [2]	2416	-
Detailed 3D analysis (bending failure)	2348	-
Design codes / analytical		
Eurocode 2 [4,5] shear or shear/torsion	2570	2405
Ultimate bending moment	2458	-

It is surprising that for beam type 101 the ultimate bending moment derived from the cross-sectional analysis results in a somewhat higher failure load then from the detailed 3D non-linear analysis. However, it has become clear that the shear failure and the bending moment failure are in fact very close together.

CONCLUSION

1. Shear or bending moment failure
   From the experiments as well as the detailed 3D non-linear analysis and the design code / analytical calculations it can be concluded that a bending moment failure is governing. However, the significant shear cracks observed during the experiment as well as the indication of yielding of the stirrups suggest a shear failure is indeed very close. In this respect the presence of the empty ducts has possibly triggered a somewhat premature bending moment failure. It can be concluded that the distance of 2.7d from the centre of the support is a near counterpoint between shear and bending failure in this case.
2. Effect partly filled ducts
   Partly filling the empty ducts with steel rods improved the resistance of the compression zone but could not prevent a bending moment like failure. For this purpose it is better to inject the empty duct with a self-compacting high strength concrete.
3. Behaviour beam 101/201 (symmetric versus non-symmetric)
   Although the non-symmetry seems marginal a significant different behaviour was observed for beam type 201. The rotation of the cross-section causes non-uniform stresses/strains across the compression zone which leads to a lower failure load as compared to the symmetric beam.
4. Behaviour experiment versus NLFEA
   The failure mode as well as the crack pattern from the experiment is in good agreement with the detailed 3D non-linear analysis. The local crushing of the concrete under the loading plate, close to the failure load, is also correctly captured. The failure load itself is somewhat underestimated possibly as a result of using a rotating crack model or the application of linear elements.

5. Behaviour experiment versus Design codes / analytical
   The shear or shear/torsion capacity calculated with Eurode, using mean values for material strength, is within the scatter of the experimental results. The calculation of the ultimate bending moment indicates a limited reduction due to the presence of the empty ducts of about 6%.

The FEM analysis of the non-symmetric beam type 201 as well as the application of different crack models, i.e. fixed crack versus rotating crack, will be part of future investigation. For beam 201 the influence of torsion as well as the ultimate bending moment will also be part of future investigation.

REFERENCES

[1] Ensink, S.W. H. Non-linear orthotropic behaviour bridge deck. Experimental measurements report. Document 25.5-14-13. Delft University of Technology. November 2014.

[2] Den Uijl, J. 2D non-linear analysis T-beam using ATENA (private communication). Delft University of Technology. 2013.

[3] Rijkswaterstaat. Guidelines for Nonlinear Finite Element Analysis of Concrete Structures. Scope: Girder Members. Technical report, The Dutch ministry of public works and the environment, The Netherlands, 2012. Document RTD 1016:2012.

[4] NEN-EN 1992-1-1+C2:2011: Eurocode 2: Design of concrete structures - Part 1-1: General rules and rules for buildings.

[5] NEN-EN 1992-1-1+C2/NB:2011: National Annex (Dutch) to NEN-EN 1992-1-1+C2:2011 Eurocode 2: Design of concrete structures - Part 1-1: General rules and rules for buildings.

[6] ATENA User manual version 5.1.1.0. Cervenka Consulting (www.cervenka.cz).

[7] DIANA User manual version 9.4.4. TNO DIANA (www.tnodiana.com). 2012.